IEEE Photonics Journal
An IEEE Photonics Society Publication

Open Access

Dispersion Engineering of Highly Nonlinear Chalcogenide Suspended-Core Fibers

Volume 7, Number 3, June 2015

E. Coscelli, Member, IEEE
F. Poli
J. Li
A. Cucinotta, Member, IEEE
S. Selleri, Senior Member, IEEE

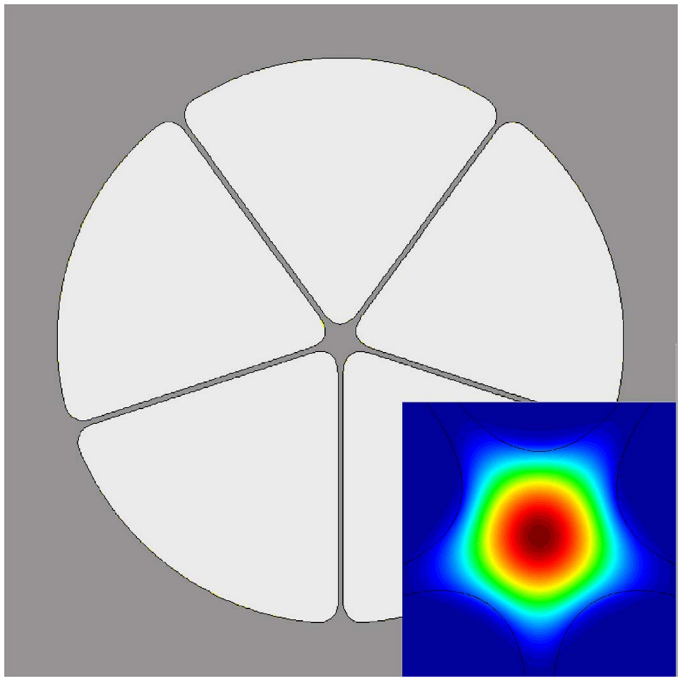

DOI: 10.1109/JPHOT.2015.2421436
1943-0655

IEEE photonics SOCIETY

IEEE

Dispersion Engineering of Highly Nonlinear Chalcogenide Suspended-Core Fibers

E. Coscelli,[1] *Member, IEEE*, F. Poli,[1] J. Li,[2,3] A. Cucinotta,[1] *Member, IEEE*, and S. Selleri,[1] *Senior Member, IEEE*

[1]Department of Information Engineering, University of Parma, 43124 Parma, Italy
[2]State Key Laboratory of Electronic Thin Films and Integrated Devices, School of Optoelectronic Information, University of Electronic Science and Technology of China, Chengdu 610054, China
[3]Institute of Photonic and Technology, Aston University, B4 7ET Birmingham, U.K.

DOI: 10.1109/JPHOT.2015.2421436

Manuscript received February 16, 2015; revised April 1, 2015; accepted April 3, 2015. Date of publication April 9, 2015; date of current version April 23, 2015. Corresponding author: E. Coscelli (e-mail: enrico.coscelli@nemo.unipr.it).

Abstract: Chalcogenide optical fibers are currently undergoing intensive investigation with the aim of exploiting the excellent glass transmission and nonlinear characteristics in the near- and mid-infrared for several applications. Further enhancement of these properties can be obtained, for a particular application, with optical fibers specifically designed that are capable of providing low effective area together with a properly tailored dispersion, matching the characteristics of the laser sources used to excite nonlinear effects. Suspended-core photonic crystal fibers are ideal candidates for nonlinear applications, providing small-core waveguides with large index contrast and tunable dispersion. In this paper, the dispersion properties of As_2S_3 suspended-core fibers are numerically analyzed, taking into account, for the first time, all the structural parameters, including the size and the number of the glass bridges. The results show that a proper design of the cladding struts can be exploited to significantly change the fiber properties, altering the maximum value of the dispersion parameter and shifting the zero-dispersion wavelengths over a range of 400 nm.

Index Terms: Optical fibers, fiber nonlinear optics.

1. Introduction

Recently, chalcogenide glass based optical devices have attracted great attention because of their potential applications in telecommunication such as signal regeneration [1], wavelength conversion in the infrared (IR) using Raman shifting [2], [3], and mid-IR SuperContinuum (SC) generation [4]–[6]. Chalcogenide glasses are based on a mixture of chalcogen elements: sulphur (S), selenium (Se), or tellurium (Te) and other elements such as arsenic, germanium, antimony, or gallium. Compared to silica glasses, they offer extraordinary nonlinear characteristics, i.e. their nonlinear refractive index can be two to three order of magnitude higher than the one of silica fiber, depending on the composition [1]. Moreover, they provide low two-photon absorption [7], and an excellent transmission window that extends far into the IR spectral region, up to 10 μm, 12 μm, and 20 μm for S, Se, and Te based glasses, respectively. However, the higher refractive index of chalcogenide glasses compared to silica leads to longer material Zero Dispersion Wavelength (ZDW) of about 4.5 μm [6]. This feature is harmful for the applications in mid-IR

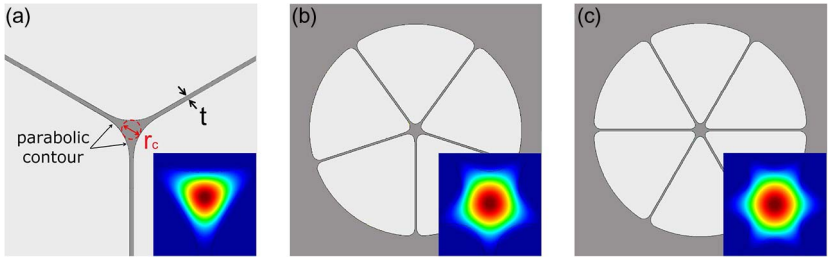

Fig. 1. (a) Detail of the core of the SCF with three bridges. Cross-section of the SCF with (b) five and (c) six bridges. Insets show the magnetic field modulus distribution of the fundamental mode, calculated at $\lambda = 2000$ nm.

non-linear optics. In fact, the large normal dispersion at telecom wavelengths distorts ultra-short optical pulses [8], and the long ZDW does not allow an anomalous dispersion pumping for broadband SC generation. To harness the useful features of chalcogenide glasses, control of chromatic dispersion while keeping low effective area must be addressed.

Suspended-Core Fiber (SCF) is an excellent candidate for further enhancing of nonlinear properties and for dispersion engineering [9], [10]. The small core and high NA of SCF ensure tight confinement of light and high nonlinearity. Besides, low loss, high air-filling fraction, and ultra low mode field diameter have attracted designers to exploit SCFs for different nonlinear applications. The most important ones for chalcogenide-made fibers at present are wavelength conversion [11], [12] and SC generation [13], [14]. Recently soliton self-frequency shift and third-harmonic generation has been measured in a four-hole tapered As_2S_5 SCF with ZDW at 1.61 μm, pumped by 1.55 μm pulsed laser [11]. Moreover, fourth order cascaded Raman wavelength shifting from 2092 nm to 2450 nm has been demonstrated in a low loss $As_{38}Se_{62}$ SCF with ZDW of 3.15 μm, pumped by 1995 nm Thulium-doped gain switched laser [12]. Finally, a mid-IR SC spanning from 1 to 4 μm has been experimentally shown in an As_2S_3 SCF with ZDW of 1660 nm pumped by an Optical Parametric Oscillator (OPO) laser with tunable wavelength from 1.7 μm to 2.6 μm [13], while one spanning from 1.5 μm to 4.5 μm has been achieved in an As_2S_3 SCF with ZDW of 2.52 μm pumped by an OPO laser with tunable wavelength from 2.2 μm to 2.6 μm [14].

As demonstrated by the above literature, it is necessary to change the suspended-core fiber chromatic dispersion and nonlinear characteristics for different pump wavelengths and applications. Several publications have already addressed the dispersion engineering of SCFs [10], [15]–[17], but a comprehensive study devoted to a thorough analysis of the effects of all the cross-section parameters on the fiber properties has yet to be presented. In particular, the effects of the number and width of the glass bridges that intersect to form the core are usually neglected, and the dispersion properties are usually related to the core diameter only. The aim of this paper is to theoretically demonstrate that the bridge parameters have a strong impact on the SCF guiding properties and can be successfully used to tailor the dispersion curve to match the requirements for specific applications. For instance, they can be used to flatten the dispersion curve or to shift the ZDWs.

2. Chalcogenide SCFs

The cross-sections of the chalcogenide SCFs considered in the present analysis, that is with three, five, and six air-holes in the cladding, separated by the same number of thin glass bridges, are shown in Fig. 1(a)–(c). The fiber core is created by the intersection of the glass bridges, linked by parabolic-shaped connectors. Notice that the cross-section has a C_n symmetry, being n the number of bridges. Since there are very few examples of SCFs with four bridges in literature, due to more severe practical issues in their fabrication, they were not studied. The guiding properties of SCFs are determined by four main cross-section parameters, that are the core radius r_c, defined as the radius of the largest circumference inscribed at the intersection of the

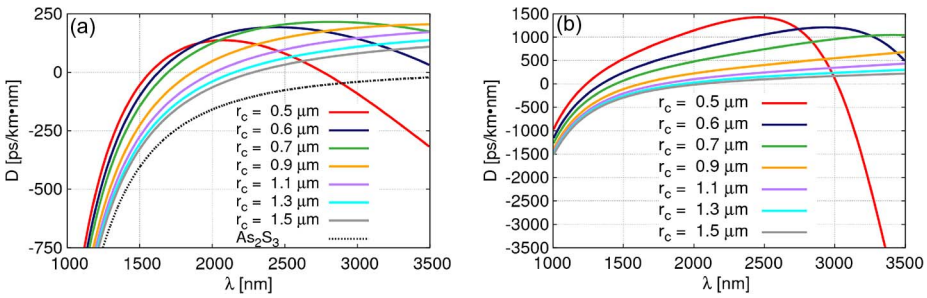

Fig. 2. Dispersion parameter D calculated (a) for SCFs with different core radius and bridge thickness $t = 0.45$ μm and (b) for glass nanowires in air with different radius.

glass bridges, the strut number and thickness t, and the glass composition, which influences material dispersion and nonlinearity. Values of r_c in the range of 0.5 μm–1.5 μm and of t between 0.15 μm and 0.45 μm have been considered. Sub-μm core chalcogenide SCF manufacturing and precise control of the size and shape of the bridges are still technologically challenging, and most of the fibers reported so far are limited to $r_c \geq 1$ μm [13], [17]. Nevertheless, fiber tapering to shrink the core radius to about 0.5 μm over few cm, which is the length required for SC generation, appears to be viable [18]. Distortions of the fiber cross-section may also arise during fabrication. A thorough analysis of their effect on the dispersion properties will be the object of future work. The length of the struts is about 20 μm, which is a typical value for manufactured SCFs. As_2S_3 chalcogenide glass has been chosen for the simulations, because of its high infrared transparency, up to 10 μm, its high nonlinear coefficient and its good drawing capability [17]. The refractive index of As_2S_3 has been calculated according to the Sellmeier equation:

$$n^2(\lambda) = 1 + \sum_i \frac{A_i \lambda^2}{\lambda^2 - \lambda_i^2} \tag{1}$$

being $A_1 = 1.8983678$, $A_2 = 1.9222979$, $A_3 = 0.8765134$, $A_4 = 0.1188704$, $A_5 = 0.9569903$, $\lambda_1^2 = 0.0225$ μm^2, $\lambda_2^2 = 0.0625$ μm^2, $\lambda_3^2 = 0.1225$ μm^2, $\lambda_4^2 = 0.2025$ μm^2, and $\lambda_5^2 = 750$ μm^2 [19]. Notice that the Sellmeier coefficients strongly depend on chalcogenide glass composition and that the values considered in this analysis are widely used as a reference in literature, even if they might change due to specific glass preparation. Nevertheless, the general trends inferred by the following study are valid for any glass.

The fundamental mode of the SCFs has been calculated in the wavelength range from 1000 nm to 3500 nm by means of a custom full-vector modal solver based on the finite-element method [20], which has been already applied with success to the analysis of the dispersion properties of several photonic crystal fibers [21]–[23]. Particular care has to be taken in the definition of the mesh at the silica-air interface, since strong field changes are expected to occur in this region, with significant impact on the dispersion properties. Examples of the calculated magnetic field modulus distribution at $\lambda = 2000$ nm are shown in the insets of Fig. 1(a)–(c).

3. Numerical Results

3.1. Dispersion Engineering

As shown by the dashed black line in Fig. 2(a), bulk As_2S_3 glass exhibits an all-normal dispersion curve throughout the considered wavelength range, which can be tailored to provide anomalous dispersion by exploiting the strong waveguide component in SCFs. The colored lines in Fig. 2(a) represent the dispersion parameter D values obtained for 3-bridge SCFs with different core radii and $t = 0.45$ μm. Notice that the fibers with larger r_c have a slope of the dispersion curve similar to the pure glass one, with D values that increase monotonically. On the contrary,

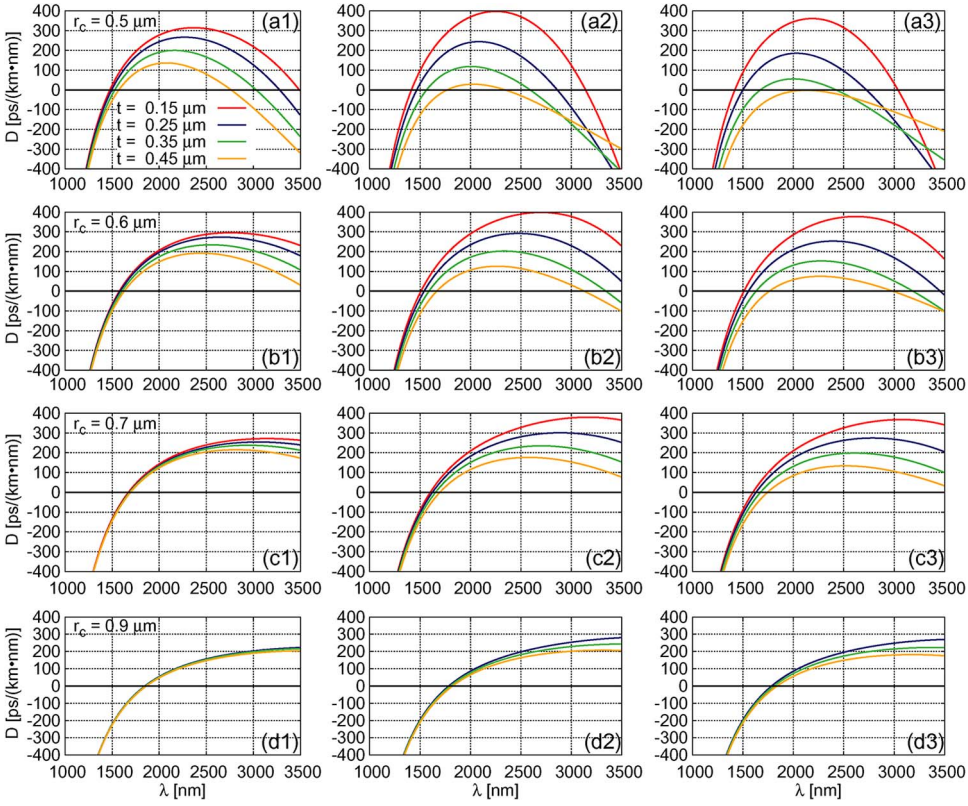

Fig. 3. Dispersion parameter versus wavelength for SCF with (top to bottom) core radius $r_c = 0.5$ μm, 0.6 μm, 0.7 μm, and 0.9 μm and (left to right) three, five, and six air-holes.

the dispersion curves of SCFs with core radius smaller than 0.9 μm have a pronounced upside-down U-shape, which yields to the appearance of a second ZDW $\lambda_{ZDW,2}$ for $r_c = 0.5$ μm, and a blue-shift of the first ZDW $\lambda_{ZDW,1}$ with decreasing r_c values. For comparison, the dispersion curve of the ideal counterpart of a SCF, that is a circular glass rod in air with the same radius of the fiber core, is shown in Fig. 2(b). It is worth noting that for large cores the dispersion of this structure resembles the one of the corresponding SCF, while it is very different when $r_c < 1$ μm. This behavior is due to the shape of the SCF core, which causes a significant overlap of the fundamental mode field with the air regions between the glass bridges, therefore altering the dispersion properties. This effect is more pronounced with a smaller core, due to the weaker guided mode field confinement in the glass. Since the core shape is a consequence of the number and width of the glass bridges, their impact on the dispersion properties, which is commonly neglected, should be taken into account. Fig. 3 demonstrates the effects of the glass bridge characteristics on the dispersion curves of SCFs with core radius between 0.5 μm and 0.9 μm. The leftmost graphs, labeled (a1)–(d1), show the results obtained for the SCFs with 3 bridges, while those in the center and rightmost columns, that is (a2)–(d2) and (a3)–(d3), report D values for the fibers with 5 and 6 bridges respectively. The general trend, which can be observed comparing the figures from top to bottom, is that the influence of the struts becomes less and less significant with increasing core radius, so that all the dispersion curves converge. If r_c is small enough, a clearly upside-down U-shaped dispersion curve is obtained, with two ZDWs in the considered wavelength range. Notice that wider struts cause an overall decrease of the dispersion parameter values, a red-shift of $\lambda_{ZDW,1}$ and a larger blue-shift of $\lambda_{ZDW,1}$. As a consequence, the two ZDWs are pulled close to each other, and between them the dispersion parameter approaches zero. It is important to underline that SCFs with five and six air-holes are even more influenced by the size of the glass bridges with respect to 3-fold ones. Indeed, the

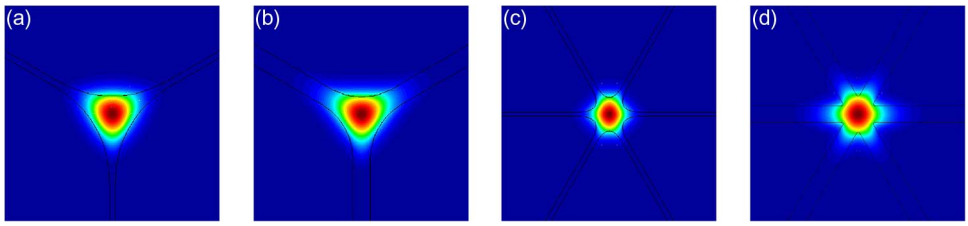

Fig. 4. Fundamental mode magnetic field modulus distribution at $\lambda = 2000$ nm for SCFs with three bridges and (a) $t = 0.15$ μm, (b) $t = 0.45$ μm, and for SCFs with six bridges and (c) $t = 0.15$ μm, (d) $t = 0.45$ μm.

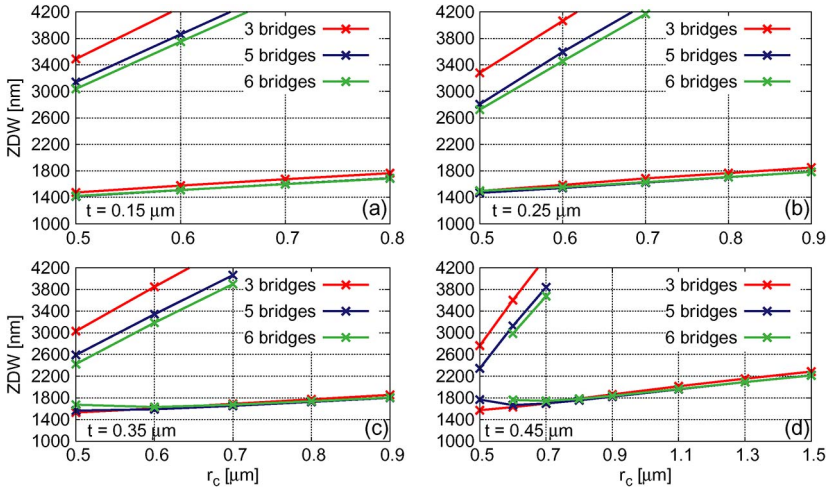

Fig. 5. Zero-dispersion wavelengths of the considered SCFs with different core radius and (a) $t = 0.15$ μm, (b) $t = 0.25$ μm, (c) $t = 0.35$ μm, and (d) $t = 0.45$ μm.

maximum value of D calculated for SCFs with five or six bridges and $t = 0.15$ μm is higher than the one obtained with the fiber with three struts, while the minimum dispersion parameter value, which is found for $t = 0.45$ μm, is lower, regardless of the core radius. The dispersion curve behavior is strictly related to the fundamental mode field confinement in the core, which is less tight for wider or more numerous struts, allowing a stronger field penetration and, consequently, emphasizing the waveguide dispersion component. This effect is demonstrated by Fig. 4(a) and (b), which report the fundamental mode field distribution of three-bridge SCFs with $r_c = 0.5$ μm, and $t = 0.15$ μm and $t = 0.45$ μm, respectively, and it is even stronger with a six-bridge geometry, as shown by Fig. 4(c) and (d). Notice that the SCF with six bridges, $r_c = 0.5$ μm and $t = 0.45$ μm has an all-normal dispersion curve in the considered wavelength range, as shown in Fig. 3(a3).

Guidelines for ZDW tuning can be inferred from Fig. 5(a)–(d). It is possible to red-shift $\lambda_{ZDW,1}$ increasing r_c or t, the former parameter playing a major role, which is only marginally influenced by the number of bridges. Through a proper combination of r_c and t values $\lambda_{ZDW,1}$ can be adjusted between 1420 nm, which is obtained with $r_c = 0.5$ μm and $t = 0.15$ μm, and 2200 nm, with $r_c = 1.5$ μm, regardless of t. $\lambda_{ZDW,1}$ can be placed at 2000 nm, a convenient wavelength for pumping with Tm-doped fiber lasers, by choosing $r_c = 1.1$ μm and $t = 0.45$ μm, regardless of the number of bridges. The change of the structural parameters can be exploited very effectively to pull a second ZDW into the considered range and to tune it. As shown in Fig. 5, $\lambda_{ZDW,2}$ rapidly red-shifts with increasing r_c, regardless of the strut number, while it can be brought closer to the first ZDW by adding more glass bridges in the fiber cross-section, for fixed r_c and t values. Indeed, a blue shift of $\lambda_{ZDW,2}$ of about 400 nm is obtained by increasing the number of

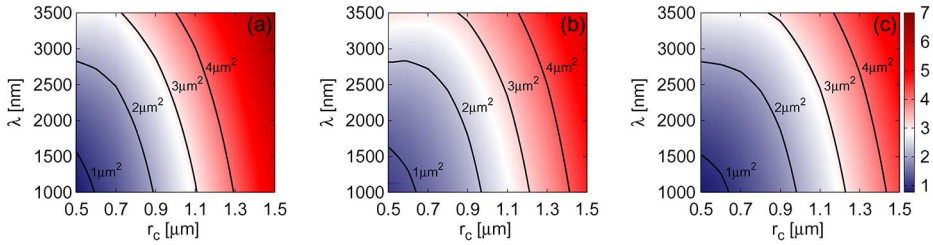

Fig. 6. Effective area as a function of core radius and wavelength for considered SCFs with (a) three bridges, (b) five bridges, and (c) six bridges, and $t = 0.45$ μm.

struts from 3 to 5, and a further shift of 100 nm can be provided by the addition of another bridge. Moreover, larger struts can be employed to push the second ZDW towards shorter wavelengths. Finally, it should be pointed out that the extreme dispersion properties of five- and six-fold SCFs with very small cores cause the two ZDWs to become very close, drifting from the almost linear dependence with core radius, down to the case of the six-fold fiber with $r_c = 0.5$ μm and $t = 0.45$ μm, which provides all-normal dispersion.

To sum up the results on the dispersion properties, it is worth noting that the design with three bridges allows to blue-shift the material ZDW by more than 3500 nm, by acting only on the values of r_c and t. SCFs with three bridges are easier to manufacture with small core diameters, without requiring tapering, and are the most used so far. The designs with five and six struts enable a stronger control of the dispersion curve, allowing dual-ZDW dispersion profiles with very close zero dispersion wavelengths and lower D values in the anomalous regime, or even all-normal dispersion curves. On the other side, manufacturing of five-fold and six-fold SCFs with small cores is more difficult. As a consequence, they should be considered only in case that a fine dispersion tailoring is required to provide a significant benefit for the desired application.

3.2. Effective Area

Besides the dispersion control, for applications such as wavelength conversion or SC generation it is important to design SCFs with low effective area and high nonlinear coefficient, in order to fully exploit the potential of the chalcogenide glass. Fig. 6(a)–(c) show the effective area A_{eff} calculated for the SCFs with $t = 0.45$ μm and three, five, and six struts, respectively, as a function of r_c. Due to the large index contrast between As_2S_3 glass and air, the effective area has been calculated according to the generalized definition [24]

$$A_{eff} = \frac{\left|\int (\bar{E} \times \bar{H}^*) \cdot \hat{z} dA\right|^2}{\int \left|(\bar{E} \times \bar{H}^*) \cdot \hat{z}\right|^2 dA} \tag{2}$$

being $\bar{E}$ and $\bar{H}$ the electric and magnetic field and the integration over the whole fiber cross-section. Notice that, due to the high refractive index of the chalcogenide glass and to the reduced dimension of the fiber core, very small effective area can be achieved, down to less than 1 μm^2 between 1000 nm and 1500 nm for the SCFs with $r_c = 0.5$ μm, regardless of the number of bridges. Unsurprisingly, for a fixed core radius, A_{eff} monotonically increases with the wavelength, as the fundamental mode field confinement worsens. Nevertheless, effective area lower than 4 μm^2 can be obtained at $\lambda = 3500$ nm, the longest wavelength considered in this analysis, in fibers with relatively large core radii, up to 1.1 μm–1.2 μm. Moreover, for all the wavelengths between 1000 nm and 3500 nm, the SCF A_{eff} increases with r_c. As a consequence, none of the considered fibers appears to have a core radius below the threshold for which any further decrease of its size causes an effective area enlargement, due to the leakage of the fundamental mode into the air-holes [10]. In general, SCFs with more struts provide a smaller A_{eff} value for a given r_c, λ pair. This is due to the fact that, as the number of bridges increases, the

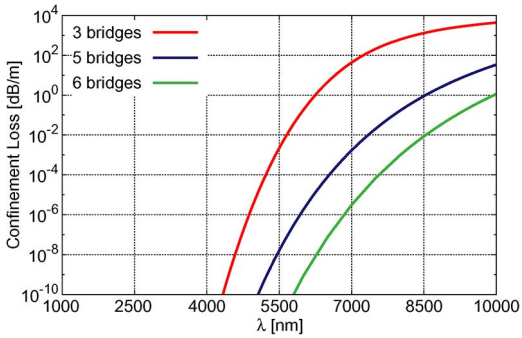

Fig. 7. Confinement loss calculated for three-, five-, and six-bridge SCFs with $r_c = 0.5$ μm and $t = 0.45$ μm.

guided mode field becomes less prone to leakage, since the intersections between core and glass struts contribute to enlarge the area available for the field confinement.

3.3. Confinement Loss

Finally, in order to deploy dispersion-engineered SCF designs for practical applications, their confinement losses in the mid-IR should be taken into account. Among the fibers considered in the present study, the most critical from this point of view are the ones with the largest t/r_c ratio, due to the fact that when the thickness of the bridges approach the core dimension, they allow a stronger leakage of the guided mode field. Therefore, confinement losses of the three-, five-, and six-bridge SCFs with $r_c = 0.5$ μm and $t = 0.45$ μm have been calculated, and are shown in Fig. 7. It is important to underline that over the whole wavelength range considered for the analysis of the dispersion properties, that is between 1000 nm and 3500 nm, losses are lower than 10^{-10} dB/m, which is below the threshold of the solver numerical error. Confinement losses approach the glass attenuation only at wavelengths beyond 5000 nm, that is outside the range taken into account for the dispersion engineering. Finally, lower losses have been obtained for SCFs with more bridges, thanks to the larger effective core area which is created by the parabolic chamfer which connects the glass struts.

4. Conclusion

The dispersion properties of As_2S_3 SCFs have been thoroughly analyzed by means of a full-vector modal solver based on the finite-element method. The possibility of widely tuning the position of the ZDWs by acting on the number and size of the glass bridges has been investigated for the first time, showing that they have an impact on the dispersion characteristics which is comparable to the one of the core size. A wide range of possible designs have been considered, providing guidelines to obtain highly nonlinear SCFs with properties suitable for several applications relying on different pump source wavelengths.

Acknowledgment

The authors wish to thank R. Dauliat, L. Brilland, and J. Troles for providing useful information about chalcogenide glasses and chalcogenide fiber fabrication.

References

[1] J. M. Harbold *et al.,* "Highly nonlinear As–S–Se glasses for all-optical switching," *Opt. Lett.*, vol. 27, no. 2, pp. 119–121, Jan. 2002. [Online]. Available: http://ol.osa.org/abstract.cfm?URI=ol-27-2-119
[2] F. Désévédavy *et al.,* "Small-core chalcogenide microstructured fibers for the infrared," *Appl. Opt.*, vol. 47, no. 32, pp. 6014–6021, Nov. 2008. [Online]. Available: http://ao.osa.org/abstract.cfm?URI=ao-47-32-6014
[3] V. Ta'eed *et al.,* "Ultrafast all-optical chalcogenide glass photonic circuits," *Opt. Exp.*, vol. 15, no. 15, pp. 9205–9221, Jul. 2007. [Online]. Available: http://www.opticsexpress.org/abstract.cfm?URI=oe-15-15-9205

[4] C. W. Rudy, A. Marandi, K. L. Vodopyanov, and R. L. Byer, "Octave-spanning supercontinuum generation in in situ tapered AS_2S_3 fiber pumped by a thulium-doped fiber laser," *Opt. Lett.*, vol. 38, no. 15, pp. 2865–2868, Aug. 2013. [Online]. Available: http://ol.osa.org/abstract.cfm?URI=ol-38-15-2865
[5] Y. Yue *et al.,* "Octave-spanning supercontinuum generation of vortices in an As_2S_3 ring photonic crystal fiber," *Opt. Lett.*, vol. 37, no. 11, pp. 1889–1891, Jun. 2012. [Online]. Available: http://ol.osa.org/abstract.cfm?URI=ol-37-11-1889
[6] C. Wei, X. Zhu, R. A. Norwood, F. Song, and N. Peyghambarian, "Numerical investigation on high power mid-infrared supercontinuum fiber lasers pumped at 3 μm," *Opt. Exp.*, vol. 21, no. 24, pp. 29488–29504, Dec. 2013. [Online]. Available: http://www.opticsexpress.org/abstract.cfm?URI=oe-21-24-29488
[7] A. Zakery and S. R. Elliott, *Optical Nonlinearities in Chalcogenide Glasses and Their Applications*. Dordrecht, The Netherlands: Springer Ser. Mater. Sci., 2007.
[8] R. E. Slusher *et al.,* "Large Raman gain and nonlinear phase shifts in high-purity As_2Se_3 chalcogenide fibers," *J. Opt. Soc. Amer. B, Opt. Phys.*, vol. 21, no. 6, pp. 1146–1155, Jun. 2004. [Online]. Available: http://josab.osa.org/abstract.cfm?URI=josab-21-6-1146
[9] S. V. Afshar, W. Q. Zhang, H. Ebendorff-Heidepriem, and T. M. Monro, "Small core optical waveguides are more nonlinear than expected: Experimental confirmation," *Opt. Lett.*, vol. 34, no. 22, pp. 3577–3579, Nov. 2009. [Online]. Available: http://ol.osa.org/abstract.cfm?URI=ol-34-22-3577
[10] H. Ebendorff-Heidepriem, S. C. Warren-Smith, and T. M. Monro, "Suspended nanowires: Fabrication, design and characterization of fibers with nanoscale cores," *Opt. Exp.*, vol. 17, no. 4, pp. 2646–2657, Feb. 2009. [Online]. Available: http://www.opticsexpress.org/abstract.cfm?URI=oe-17-4-2646
[11] T. Cheng *et al.,* "Soliton self-frequency shift and third-harmonic generation in a four-hole As_2S_5 microstructured optical fiber," *Opt. Exp.*, vol. 22, no. 4, pp. 3740–3746, Feb. 2014. [Online]. Available: http://www.opticsexpress.org/abstract.cfm?URI=oe-22-4-3740
[12] M. Duhant *et al.,* "Fourth-order cascaded Raman shift in AsSe chalcogenide suspended-core fiber pumped at 2 μm," *Opt. Lett.*, vol. 36, no. 15, pp. 2859–2861, Aug. 2011. [Online]. Available: http://ol.osa.org/abstract.cfm?URI=ol-36-15-2859
[13] I. Savelii *et al.,* "Mid-infrared 2000-nm bandwidth supercontinuum generation in suspended-core microstructured sulfide and tellurite optical fibers," *Opt. Exp.*, vol. 20, no. 24, pp. 27083–27093, Nov. 2012. [Online]. Available: http://www.opticsexpress.org/abstract.cfm?URI=oe-20-24-27083
[14] W. Gao *et al.,* "Mid-infrared supercontinuum generation in a suspended-core As_2S_3 chalcogenide microstructured optical fiber," *Opt. Exp.*, vol. 21, no. 8, pp. 9573–9583, Apr. 2013. [Online]. Available: http://www.opticsexpress.org/abstract.cfm?URI=oe-21-8-9573
[15] C. Chaudhari, T. Suzuki, and Y. Ohishi, "Design of zero chromatic dispersion chalcogenide As_2S_3 glass nanofibers," *J. Lightw. Technol.*, vol. 27, no. 12, pp. 2095–2099, Jun. 2009. [Online]. Available: http://jlt.osa.org/abstract.cfm?URI=jlt-27-12-2095
[16] M. Szpulak and S. Fevrier, "Chalcogenide As_2S_3 suspended core fiber for mid-IR wavelength conversion based on degenerate four-wave mixing," *IEEE Photon. Technol. Lett.*, vol. 21, no. 13, pp. 884–886, Jul. 2009.
[17] M. El-Amraoui *et al.,* "Strong infrared spectral broadening in low-loss As–S chalcogenide suspended core microstructured optical fibers," *Opt. Exp.*, vol. 18, no. 5, pp. 4547–4556, Mar. 2010. [Online]. Available: http://www.opticsexpress.org/abstract.cfm?URI=oe-18-5-4547
[18] W. Gao *et al.,* "Visible light generation and its influence on supercontinuum in chalcogenide As_2S_3 microstructured optical fiber," *Appl. Phys. Exp.*, vol. 4, no. 10, Oct. 2011, Art. ID. 102601. [Online]. Available: http://stacks.iop.org/1882-0786/4/i=10/a=102601
[19] W. Rodney, I. Malitson, and T. King, "Refractive index of arsenic trisulfide," *J. Opt. Soc. Amer.*, vol. 48, no. 9, pp. 633–636, Sep. 1958.
[20] F. Poli, A. Cucinotta, and S. Selleri, *Photonic Crystal Fibers. Properties and Applications*. Dordrecht, The Netherlands: Springer Ser. Mater. Sci., 2007.
[21] F. Poli, A. Cucinotta, S. Selleri, and A. Bouk, "Tailoring of flattened dispersion in highly nonlinear photonic crystal fibers," *IEEE Photon. Technol. Lett.*, vol. 16, no. 4, pp. 1065–1067, Apr. 2004.
[22] A. Bouk, A. Cucinotta, F. Poli, and S. Selleri, "Dispersion properties of square-lattice photonic crystal fibers," *Opt. Exp.*, vol. 12, no. 5, pp. 941–946, Mar. 2004.
[23] F. Poli, A. Cucinotta, M. Fuochi, S. Selleri, and L. Vincetti, "Characterization of microstructured optical fibers for wideband dispersion compensation," *J. Opt. Soc. Amer. A, Opt. Image Sci.*, vol. 20, no. 10, pp. 1958–1962, Oct. 2003.
[24] S. Afshar and T. M. Monro, "A full vectorial model for pulse propagation in emerging waveguides with subwavelength structures part 1: Kerr nonlinearity," *Opt. Exp.*, vol. 17, no. 4, pp. 2298–2316, Feb. 2009.